LIQUID CRYSTALS
2019, VOL. 46, NO. 2, 309–315
https://doi.org/10.1080/02678292.2018.1499971

Taylor & Francis
Taylor & Francis Group

High-frame-rate liquid crystal phase modulator for augmented reality displays

Ran Chen[a,b], Yuge Huang[b], Jian Li[c], Minggang Hu[c], Juanli Li[c], Xinbing Chen[a], Pei Chen[a], Shin-Tson Wu[b] and Zhongwei An[a,c]

[a]Key Laboratory of Applied Surface and Colloid Chemistry, School of Materials Science and Engineering, Shaanxi Normal University, Xi'an, China; [b]College of Optics and Photonics, University of Central Florida, Orlando, FL, USA; [c]Optical and Electrical Material Center, Xi'an Modern Chemistry Research Institute, Xi'an, China

ABSTRACT

We optimise a new liquid crystal mixture with wide nematic range, high birefringence (Δn), high resistivity, moderate dielectric anisotropy ($\Delta\varepsilon$) and relatively low rotational viscosity for augmented reality display applications. High Δn and large $\Delta\varepsilon$ allow a thin cell gap ($d \approx 1.5$ μm) to be employed in a reflective liquid-crystal-on-silicon (LCoS) device to achieve 2π phase change at 5 V and 2.87 ms average phase-to-phase response time at 40°C without complicated overdrive circuitry. Such a fast response time enables an LCoS panel to achieve 240 Hz frame rate for field sequential colour operation to avoid image flickering.

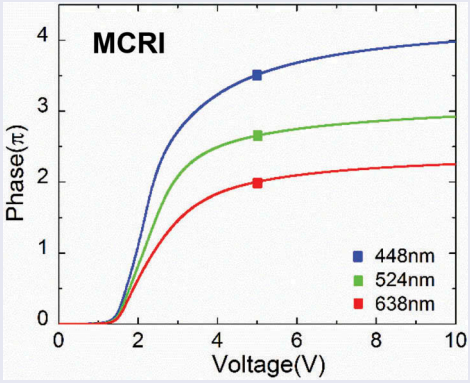

ARTICLE HISTORY
Received 26 February 2018
Accepted 9 July 2018

KEYWORDS
Spatial light modulators; liquid crystals; high birefringence; AR display

1. Introduction

Liquid-crystal-on-silicon (LCoS) panel has been widely used for intensity modulation in augmented reality (AR) displays, such as Google Glass and Microsoft HoloLens, because of its high resolution, low driving voltage and low power consumption [1–3]. To overcome the focus-cue mismatch issue, phase-only LCoS has found useful applications in focal surface displays [4–6]. For these applications, a large phase modulation depth (≥2π) is required. Meanwhile, the liquid crystal (LC) response time should be less than 4 ms in order to achieve the desired 240 Hz frame rate. From [4,5], both Oculus and Microsoft devices were operated at 60 Hz, which is 4 times too slow to meet the required 240 Hz. Therefore, there is urgent need to develop a phase-only LCoS device with response time less than 4 ms, while keeping a 2π phase change and low operation voltage (<6 V) without the overdrive and undershoot driving circuitry [7].

To improve response time, several approaches have been investigated, such as dual-frequency LCs [8], polymer-stabilised blue-phase LCs [9–11], ferroelectric LCs [12,13] and polymer network LCs [14,15]. Each technology has its own pros and cons, and it is still quite challenging to satisfy all the above-mentioned requirements. For example, the complicated driving scheme of dual-frequency LCs, the high operation voltage of polymer-stabilised LCs and the bistability of ferroelectric LCs remain to be solved for LCoS-based phase modulators. Lately, a low viscosity and negative dielectric anisotropy ($\Delta\varepsilon$) LC mixture has been developed to achieve submillisecond response time for VA LCoS intensity modulator by using a thin cell gap

CONTACT Shin-Tson Wu swu@ucf.edu; Zhongwei An gmecazw@163.com
Supplemental data for this article can be accessed here.

($d \approx 1.2$ μm) [7]. However, to achieve 2π phase change, its response time would increase by 4 times, because the required cell gap is twice thicker than that of the corresponding intensity modulator. Recently, three positive $\Delta\varepsilon$ and low-viscosity LC mixtures with fast response time have been reported for 240 Hz phase-only LCoS devices [16], but their resistivity remains to be improved, which determines the voltage holding ratio in operation. These two reports employed low γ_1/K_{11} LCs to improve the response time for the applications of LCoS devices. Another common way is to use a high Δn LC to reduce cell gap for achieving faster response time. However, the high melting point and large viscosity of high Δn LC mixtures are concerns for LCoS-based phase modulators.

In this article, we reported two high Δn LC mixtures and one commercial high Δn LC mixture to know how material parameters affect the LC response time in LCoS-based phase modulators. Finally, we optimised a new nematic LC mixture, designated as MCRI, for LCoS-based phase modulators to achieve fast response time without the need of overdrive circuitry. MCRI exhibits a high birefringence ($\Delta n \sim 0.28$ at $T = 25$°C and $\lambda = 550$ nm), moderate rotational viscosity and dielectric anisotropy ($\Delta\varepsilon \sim 7.6$). By using a thin cell gap ($d \approx 1.5$ μm), we can achieve 2π phase change at 5 V and 240 Hz frame rate. Therefore, MCRI is expected to find useful applications for the emerging AR displays.

2. Material development

2.1 Components

As shown in Table 1, fluorine-containing diphenyl acetylene type LCs (#1-#3) [17], new diluter (#6) [18] and new highly fluorinated LCs (#7, #8) [19,20] were synthesised according to similar literature procedures. Here, R represents different alkyl chain. The tolane LCs (#4, #5) were purchased from Xi'an Caijing Opto-Electrical Science Technology and used as received. The commercial high Δn LC mixture (HTD028200-200) was purchased from Jiangsu Hecheng Advanced Materials and also used as received. The phase transition temperatures were measured by differential scanning calorimetry (DSC, TA instruments Q100) in nitrogen at the heating and cooling rate of 2°C min^{-1}, and POM, LEICA DM2500P with Linkam THMS600 hot-stage and control unit at a heating and cooling rate of 0.5°C min^{-1}. The phase transition temperatures reported in this article were the peak values of the transition on DSC curves.

Table 1. Chemical structures of our LC mixtures.

No.	Structures	Melting points (°C)[a]	Clearing points (°C)[a]
1	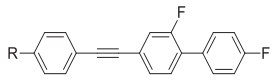	80.0	163.5
2	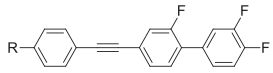	59.5	118.4
3	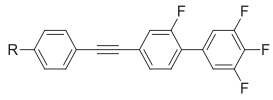	55.0	64.4
4	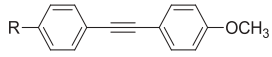	66	-
5	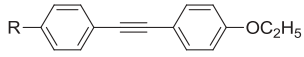	53.1	81.1
6	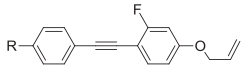	33.6	39.2
7	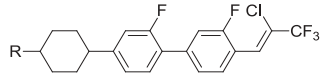	54.4	106.0
8	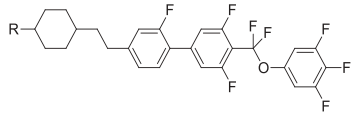	53.8	114.6

[a]The alkyl chain of each compound is *n*-propyl, except that of compound #5 represents *n*-butyl.

2.2 LC mixtures formulation

To obtain high resistivity and low viscosity simultaneously, fluorinated tolane is a good candidate. Therefore, a high Δn and high resistivity LC mixture was prepared by our synthetic compounds #1-#5 (SNNU-1): its physical properties are listed as follows: $\Delta n = 0.337$ at $\lambda = 550$ nm, $\Delta\varepsilon = 2.86$, visco-elastic constant $\gamma_1/K_{11} = 17.5$ ms/μm^2, high resistivity> 10^{13} Ω· cm, melting temperature $T_m = -18$°C and clearing temperature $T_c = 123$°C. Its birefringence is reasonably high, but its $\Delta\varepsilon$, rotational viscosity γ_1 and melting point still need improvement.

To reduce melting point and γ_1, we added 15.0 wt% of a new diluter (#6) to SNNU-1. Firstly, to maintain high Δn and increase $\Delta\varepsilon$, we attempted a high Δn

(0.21), large $\Delta\varepsilon$ (20.4) and relatively low viscosity (151.7 mPa· s) LC (#7), while it was difficult to blend in the LC mixture. After optimisation, to maintain high resistivity and increase $\Delta\varepsilon$, we added 20.2 wt% of thin-film-transistor (TFT) LC (#8) with a relatively low Δn (0.14), large $\Delta\varepsilon$ (25.8), relatively large viscosity (360.0 mPa· s) and good solubility to prepare a new LC mixture MCRI (compounds #1-#6, #8).

Meanwhile, we selected a commercial LC mixture (HTD028200-200) for comparison (not listed in Table 1). As a common issue for high Δn and large $\Delta\varepsilon$ LC mixtures, its relatively low resistivity ($> 2 \times 10^{11}$) hinders its application for phase LCoS. Another general concern for high Δn LC materials is their UV stability [21,22]. To prevent photo-degradation, we recommend blocking the LC area from UV exposure during sealing process.

3. Material characterisation

Table 2 lists the measured physical properties of the three LC mixtures. The measurement was conducted at 40°C – the actual operating temperature of a working LCoS device, due to the thermal effects of backplane and illumination light [23].

3.1 Birefringence

To measure Δn, each LC mixture was injected into a homogeneous cell with cell gap $d \approx 5$ μm. The pretilt angle of the rubbed polyimide alignment layers is about 3°. The cell was mounted in a Linkam LTS 350 Large Area Heating/Freezing Stage controlled by TMS94 Temperature Programmer and then sandwiched between two crossed polarisers. A 1 kHz square-wave AC voltage was applied to the LC cell. The birefringence was calculated from the measured phase retardation [24]. Figure 1(a) depicts the temperature-dependent birefringence at λ = 633 nm (He-Ne laser). At λ = 633 nm and 40°C, the Δn of [SNNU-1, MCRI, HTD028200-200] is [0.2810, 0.2531, 0.2719], respectively (Table 2). The extrapolated birefringence Δn_0 at T = 0 K and the exponent β were obtained by fitting the experimental data with Equation (1) [25] and the results are listed in Table S1.

$$\Delta n = \Delta n_0 S = \Delta n_0 (1 - T/T_c)^{\beta}. \quad (1)$$

Moreover, to investigate the electro-optic performance at different colours, a tunable Argon ion laser (λ = 457, 488 and 514 nm) and a He-Ne laser (λ = 633 nm) were used for the characterisation. We fitted the measured wavelength-dependent Δn (dots in Figure 1(b)) with the single-band birefringence dispersion equation [26]:

$$\Delta n = G \frac{\lambda^2 \lambda^{*2}}{\lambda^2 - \lambda^{*2}}, \quad (2)$$

where G is a proportionality constant and λ^* is the mean resonance wavelength. The obtained G and λ^* values are listed in Table S1.

Table 2. Measured physical properties of three LC mixtures at T = 40°C.

LC mixture	T_m (°C)	T_c (°C)	Δn at 633 nm	$\Delta\varepsilon$	γ_1/K_{11}	γ_1 (mPa· s)	K_{11} (pN)
SNNU-1	−18.2	123.3	0.2810	2.59	8.58	120.1	14.0
MCRI	−38.3	107.4	0.2531	6.65	8.70	132.9	15.3
HTD028200-200	−20.1	103.2	0.2719	6.83	11.55	109.7	9.5

3.2 Visco-elastic coefficient

The rotational viscosity γ_1 and splay elastic constant [K_{11}] were measured through transient current method by autronic-MELCHRS LCCS107. We also measured the transient decay curves of these LC mixtures and obtained the temperature-dependent visco-elastic coefficient γ_1/K_{11}, as the dots presented in Figure 2. The solid lines represent fittings with following relation [27]:

$$\frac{\gamma_1}{K_{11}} = A \frac{\exp(E_a/k_B T)}{(1 - T/T_c)^{\beta}}. \quad (3)$$

In Equation (3), A, E_a and k_B stand for the proportionality constant, Boltzmann constant and activation energy, respectively. The fitting parameters used in Figures 1 and 2 are summarised in Table S1.

3.3 Dielectric anisotropy

The dielectric constants were measured with a multi-frequency LCR meter HP-4274 and results are listed in Table 2. Compared with SNNU-1, MCRI has a larger $\Delta\varepsilon$, higher γ_1 and lower Δn. The larger $\Delta\varepsilon$ helps to lower the operation voltage, but the multiple polar groups in component #8 dramatically increase γ_1 and decrease Δn [28], which would increase the response time. Herein, there is a trade-off between low voltage and fast response time.

3.4 Overall performance

Keeping a 2π phase change at low operation voltage ($V_{2\pi}$ = 5V), we used the physical parameters of three LC mixtures to simulate the response time in a

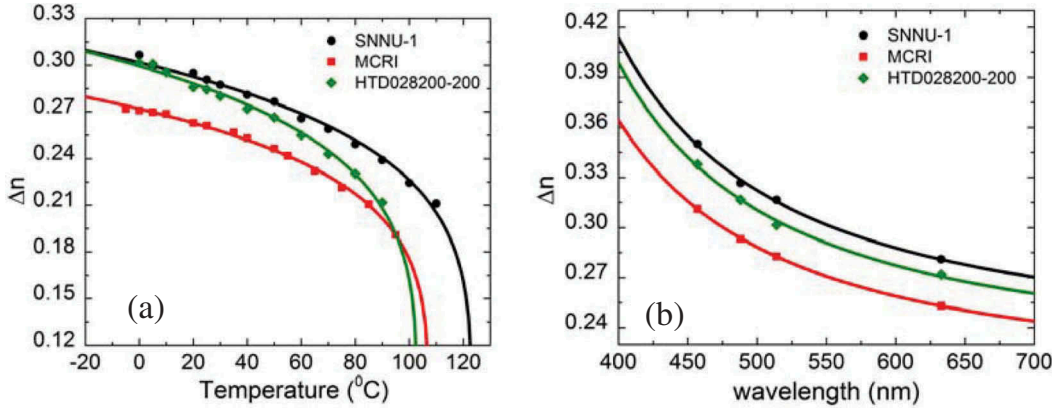

Figure 1. (Colour online) (a) Temperature-dependent birefringence at λ = 633 nm. (b) Birefringence dispersion at 40°C. Dots are measured data, and the lines in (a) and (b) are fitting curves with Equations (1) and (2), respectively.

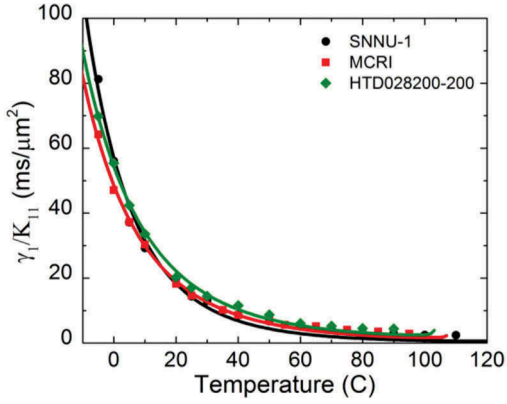

Figure 2. (Colour online) Temperature-dependent visco-elastic coefficient at λ = 633 nm. Dots are measured data and lines are fitting curves with Equation (3).

reflective cell by a commercial LCD software DIMOS 2.0. The simulated response time (rise + decay) of SNNU-1, MCRI and HTD028200-200 is 4.14, 3.14 and 3.23 ms, respectively. As expected, MCRI with a high birefringence, moderate rotational viscosity and dielectric anisotropy ($\Delta\varepsilon$ ~ 6.65) exhibits the fastest response time among the three mixtures studied. Along with its high resistivity and wide nematic range, MCRI satisfies the requirements of 240-Hz phase-only LCoS for AR displays. In the following sections, our evaluation will be focused on MCRI.

4. Device performances

4.1 Voltage-dependent phase change (VΦ) curve

To simulate the electro-optic performance of MCRI in a real LCoS device, we injected our LC mixture MCRI into a transmissive homogeneous cell with cell gap $d \approx 3.43$ μm. Then, we measured its voltage-dependent transmittance (VT) curve and converted the measured VT curve to voltage-dependent phase (VΦ) curve. The phase change of this transmissive cell is equivalent to that of a reflective cell with $d \approx 1.715$ μm, because of the doubled optical path. Figure 3 compares the VΦ curves converted from the measured VT curve (dots) with the simulated VT curve (red line). Results indicate that the simulated curve fits reasonably well with the experimental data. Therefore, the simulated VΦ curves can be used for further analysis.

4.2 Response time

As shown in Figure 3, we obtained ~ 2.21π phase change at 5V with a 3.43-μm transmissive cell. These values indicate a 2π phase change can be obtained at 5V with a 1.55-μm reflective cell. Because the response time (τ) is proportional to d^2 [29], the response time of the 1.55-μm reflective cell should be 4.9× faster than that of the 3.43-μm transmissive cell. To validate the conversion, we compared the simu-

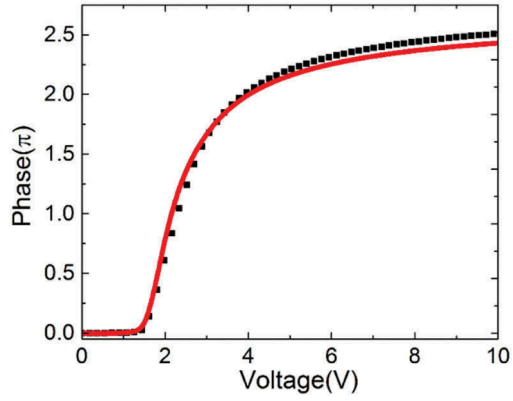

Figure 3. (Colour online) A VΦ curve of MCRI. Dots are measured data from a transmissive homogenous cell with d = 3.43 μm; the line is a simulated curve in a reflective homogenous cell with d = 1.715 μm.

Table 3. Extrapolated PTP response time of MCRI of a 1.55-μm reflective LCoS panel based on the measured data from a 3.43-μm transmissive cell.

	Rise time (ms)								
Decay time (ms)	1	2	3	4	5	6	7	8	9
1	*	15.43	9.27	5.96	4.42	3.28	2.27	1.31	0.63
2	2.48	*	6.42	3.78	3.55	2.69	1.89	1.05	0.54
3	2.38	7.75	*	3	3.16	2.4	1.69	0.97	0.49
4	2.38	6.73	4.68	*	2.86	2.2	1.54	0.89	0.45
5	2.38	6.18	4.57	3.28	*	2.01	1.36	0.84	0.42
6	2.35	5.62	4.04	3.13	2.41	*	1.33	0.81	0.41
7	2.34	5.17	3.7	2.93	2.35	1.79	*	0.79	0.4
8	2.34	4.85	3.17	2.83	2.26	1.8	1.1	*	0.39
9	2.32	4.56	3.37	2.72	2.21	1.75	1.05	0.76	*

Note: * no data.

lated response time ([rise, decay] = [0.60 ms, 2.54 ms]) of the 1.55-μm cell with the experimentally extrapolated response time ([rise, decay] = [0.63 ms, 2.32 ms]). The difference is only 6.4%.

In an AR device, each pixel of the LCoS panel should be able to generate any phase level between 0 and 2π. To evaluate the grayscale phase response, we divided the phase change into nine levels for further evaluation. Table S2 lists the representative phase levels and the corresponding operation voltages. By measuring the response time between every two phase levels, we can obtain a phase-to-phase (PTP) response time chart as shown in Table 3. The extrapolated average PTP response time of a 1.55-μm reflective LCoS panel is 2.87 ms. That means, the LCoS employing our MCRI mixture can achieve 240 Hz for field sequential colour operation.

Fast response time is indeed achieved under our thin cell strategy. However, manufacturing yield decreases as the cell gap gets thinner. The 1.55-μm cell gap is still manageable for LCoS panels. Other important parameters affecting the LCoS performance are fringing field effect and diffraction effect, especially when the pixel size is small [30]. Fringing field effect, which depends on the LC alignment, e.g. vertical alignment, twisted alignment and homogeneous alignment, have been investigated extensively [31]. A thinner cell gap is helpful to suppress the fringing field effect [30,31].

4.3 A full-colour phase-only SLM device

MCRI can also be used in a full-colour phase-only SLM device. In the Microsoft's LCoS-based AR prototypes [4], the wavelengths of the three employed laser diodes are 448, 524 and 638 nm. Therefore, in our simulation, we also chose the same wavelengths. From Figure 1(b) and Equation (2), the Δn at 40°C and λ = [448 nm, 524 nm, 638 nm] is [0.3171, 0.2790, 0.2522]. The cell gap was set at 1.52 μm to ensure $V_{2\pi} \leq 5$V works for the RGB colours. Figure 4 shows the simulated VΦ curves of MCRI for the RGB wavelengths. For red light with the longest λ and the lowest Δn, its $V_{2\pi}$ is controlled at 5 V. For the other two colours, more than 2π phase change can be obtained at 5 V.

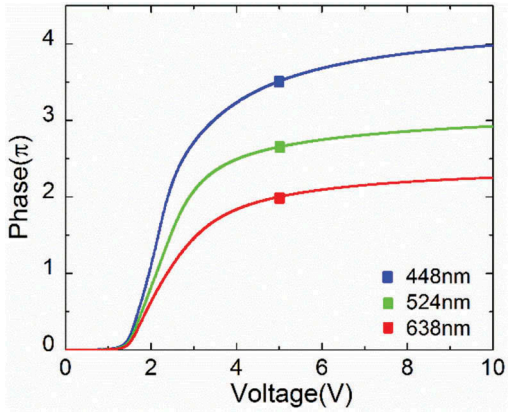

Figure 4. (Colour online) Simulated VΦ curves of MCRI for the specified RGB colours at 40°C in a reflective homogenous cell with d = 1.52 μm. Lines are VΦ curves; dots represent the upper limit of the phase change range with 5 V.

4.4 Photostability of MCRI under blue light

For a full-colour phase-only SLM device, red (λ = 638 nm), green (λ = 524 nm) and blue (λ = 448 nm) are the three primary colours. The low-energy red and green photons are much less harmful than the high-energy blue photons. Thus, the photostability of a LC mixture in practical use is determined by the blue light. Taking a 10,000-nits high-brightness backlight unit, for example, the blue light intensity on LCoS panel is about 10 mW/cm^2. After 200 working hours, the accumulated dose per unit surface area is 7.2 kJ/cm^2. To evaluate the photostability, we injected MCRI into a 5.0-μm-thick homogeneous cell and illuminated it at 40°C by a Helium-Cadmiun laser (λ = 445 nm). We monitored and recorded the birefringence (Δn) and visco-elastic coefficient (γ_1/K_{11}) of MCRI after blue light exposure. As shown in Figure 5, no obvious sign of

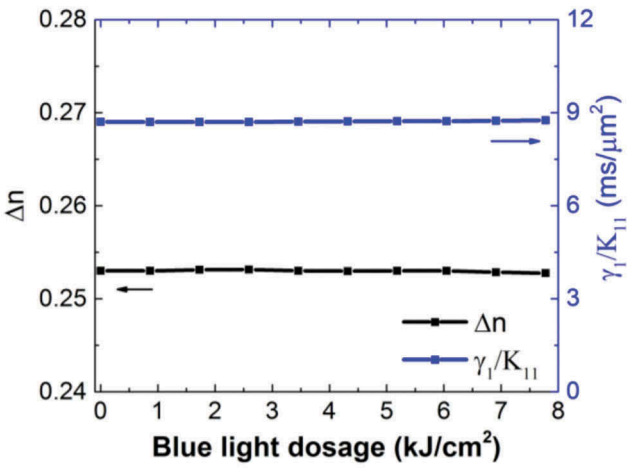

Figure 5. (Colour online) Measured photo-stability of MCRI exposed at λ = 446 nm and 40°C. Probing laser beam: λ = 633 nm. Measurement temperature: 40°C. Black dots denote birefringence and blue dots denote visco-elastic constant.

degradation of MCRI is observed after up to ~ 8 kJ/cm^2 of laser irradiation.

5. Conclusions

We have developed a new LC mixture (MCRI) for phase-only LCoS based AR displays. MCRI exhibits following physical properties: Δn = 0.253, $\Delta\varepsilon$ = 6.65, γ_1/K_{11} = 8.7 ms/μm^2 at λ = 633 nm and T = 40°C. When employing MCRI in a phase-only LCoS for AR displays, the average PTP response time is 2.87 ms, which enables 240 Hz frame rate for field sequential colour operation, while keeping a 2π phase change, 5V operation voltage and high resistivity. Potential application of MCRI for the emerging AR displays is foreseeable.

Acknowledgments

The authors would like to thank Yun-Han Lee, Dr. Haiwei Chen and Fangwang Gou for technical support and helpful discussions.

Disclosure statement

No potential conflict of interest was reported by the authors.

Funding

The Xi'an group would like to thank the Defense Industrial Technology Development Program of China (B0520132007, B1120132028), Joint Fund of Ministry of Education (6141A02022219), National Science Foundation Committee of China (21673134, 21543012) and the Fundamental Research Funds for the Central Universities (GK201704008) for financial support of this work. The UCF group is indebted to Air Force Office of Scientific Research (AFOSR) for the financial support, under grant no. FA9550-14-1-0279.

References

[1] Li YW, Lin CW, Chen KY, et al. Front-lit LCOS for wearable applications. SID Int Symp Dig Tech Pap. 2014;45(1):234–236.
[2] Cuypers D, Smet HD, Calster AV. VAN LCOS micro-displays: a decade of technological evolution. J Disp Technol. 2011;7(3):127–134.
[3] Luo Z, Peng F, Chen H, et al. Fast-response liquid crystals for high image quality wearable displays. Opt Mater Express. 2015;5(3):603–610.
[4] Maimone A, Georgiou A, Kollin JS. Holographic near-eye displays for virtual and augmented reality. ACM Trans Graph. 2017;36(4):1–16.
[5] Matsuda N, Fix A, Lanman D. Focal surface displays. ACM Trans Graph. 2017;36(4):1–14.
[6] Sun P, Chang S, Zhang S, et al. Computer-generated holographic near-eye display system based on LCoS phase only modulator. Proc SPIE. 2017;10396:103961J.
[7] Chen H, Gou F, Wu ST. Submillisecond-response nematic liquid crystals for augmented reality displays. Opt Mater Express. 2017;7(1):195–201.
[8] Xianyu H, Wu ST, Lin CL. Dual frequency liquid crystals: A review. Liq Cryst. 2009;36(6–7):717–726.
[9] Peng F, Lee YH, Luo Z, et al. Low voltage blue phase liquid crystal for spatial light modulators. Opt Lett. 2015;40(21):5097–5100.
[10] Huang Y, Chen H, Tan G, et al. Optimized blue-phase liquid crystal for field-sequential-color displays. Opt Mater Express. 2017;7(2):641–650.
[11] Tan G, Lee YH, Gou F, et al. Review on polymer-stabilized short-pitch cholesteric liquid crystal displays. J Phys D Appl Phys. 2017;50(49):493001.
[12] Srivastava K, Chigrinov VG, Kwok HS. Ferroelectric liquid crystals: excellent tool for modern displays and photonics. J Soc Inf Disp. 2015;23(6):253–272.
[13] Knust S, Wahle M, Kitzerow HS. Ferroelectric liquid crystals in microcapillaries: observation of different electro-optic switching mechanisms. J Phys Chem B. 2017;121(19):5110–5115.
[14] Chien CY, Hsu CJ, Chen YW, et al. Holographic polymer networks formed in liquid crystal phase modulators via a He-Ne laser to achieve ultra-fast optical response. Opt Express. 2016;24(7):7534–7542.
[15] Sun J, Wu ST. Recent advances in polymer network liquid crystal spatial light modulators. J Polym Sci, Part B: Polym Phys. 2014;52(3):183–192.
[16] Huang Y, He Z, Wu ST. Fast-response liquid crystal phase modulators for augmented reality displays. Opt Express. 2017;25(26):32757–32766.
[17] Li J, Yang X, Gan N, et al. The effect of lateral fluorination on the properties of phenyl-tolane liquid crystals. Liq Cryst. 2015;42(3):397–403.
[18] An Z, Chen R, Zhao L, et al. Shaanxi normal university. Side fluorine substituent and terminal alkenyl substituent-containing diphenyl acetylene diluents for high-

birefringence liquid crystals, and synthesis method thereof. Chinese patent CN 107628932. 2018 Jan 26.
[19] Li J, Hu M, Li J, et al. Highly fluorinated liquid crystals with wide nematic phase interval and good solubility. Liq Cryst. 2014;41(12):1783–1790.
[20] Song K, Li J, Li J, et al. New terphenyl liquid crystals terminated by 2-chloro-3,3,3-trifluoropropenyl group. Liq Cryst. 2017;44(11):1646–1652.
[21] Chen R, An Z, Wang W, et al. Improving UV stability of tolane-liquid crystals in photonic applications by the ortho fluorine substitution. Opt Mater Express. 2016;6 (1):97–105.
[22] Gauza S, Wang H, Wen CH, et al. High birefringence isothiocyanato tolane liquid crystals. Jpn J Appl Phys. 2003;42(6A):3463–3466.
[23] Haller I. Thermodynamic and static properties of liquid crystals. Prog Solid State Chem. 1975;10 (2):103–118.
[24] Wu ST, Efron U, Hess LD. Birefringence measurements of liquid crystals. Appl Opt. 1984;23(21):3911–3915.
[25] Beeson K, Zimmerman S, Livesay W, et al. LED-based light-recycling light sources for projection displays. SID Int Symp Dig Tech Pap. 2006;37(1):1823–1826.
[26] Wu ST. Birefringence dispersions of liquid crystals. Phys Rev A. 1986;33(2):1270–1274.
[27] Wu ST, Wu CS. Experimental confirmation of Osipov-Terentjev theory on the viscosity of liquid crystals. Phys Rev A. 1990;42(4):2219–2227.
[28] Chen R, Jiang Y, Li J, et al. Dielectric and optical anisotropy enhanced by 1,3-dioxolane terminal substitution on tolane-liquid crystals. J Mater Chem C. 2015;3(33):8706–8711.
[29] Wu ST. Design of a liquid crystal based tunable electro-optic filter. Appl Opt. 1989;28(1):48–52.
[30] Vanbrabant PJM, Beeckman J, Neyts K, et al. Diffraction and fringing field effects in small pixel liquid crystal devices with homeotropic alignment. J Appl Phys. 2010;108:083104.
[31] Fan Chiang KH, Wu ST, Chen SH. Fringing-field effects on high-resolution liquid crystal microdisplays. J Display Technol. 2005;1(2):304–313.